 doi:10.20944/preprints202107.0007.v1

Article

Conversion of Bivalve Shells to Advanced Calcium Phosphate Materials: A Simple, Rapid, Environmentally Benign, and Cost-effective Approach to Recycle Seafood Wastes

Somkiat Seesanong [1], Banjong Boonchom [2,3,*], Kittichai Chaiseeda [4,*], Wimonmat Boonmee [5] and Nongnuch Laohavisuti [6]

[1] Department of Plant Production Technology, Faculty of Agricultural Technology, King Mongkut's Institute of Technology Ladkrabang, Bangkok 10520, Thailand; ksesomki@yahoo.com
[2] Advanced Functional Phosphate Material Research Unit, Department of Chemistry, Faculty of Science, King Mongkut's Institute of Technology Ladkrabang, Bangkok 10520, Thailand; kbbanjon@gmail.com
[3] Municipal Waste and Wastewater Management Learning Center, Faculty of Science, King Mongkut's Institute of Technology Ladkrabang, Bangkok 10520, Thailand
[4] Organic Synthesis, Electrochemistry and Natural Product Research Unit (OSEN), Department of Chemistry, Faculty of Science, King Mongkut's University of Technology Thonburi, Bangkok 10140, Thailand; kittichai@gmail.com
[5] Department of Biology, Faculty of Science, King Mongkut's Institute of Technology Ladkrabang, Bangkok 10520, Thailand; bwimonmat@gmail.com
[6] Department of Animal Production Technology and Fishery, Faculty of Agricultural Technology, King Mongkut's Institute of Technology Ladkrabang, Bangkok 10520, Thailand; nongnuch.la@kmitl.ac.th

*,** Correspondence: kbbanjon@gmail.com (B.B.); kittichai@gmail.com (K.C.)

Abstract: The search for sustainable resources remains a subject of global interest and the conversion of the abundantly available bivalve shell wastes to advanced materials is an intriguing method. By grinding, each shell of bivalves (cockle, mussel, and oyster) was transformed to the same crystal type of calcite phase of $CaCO_3$, revealed by FTIR and XRD results. Each individual shell powder was reacted with H_3PO_4 and H_2O to prepare $Ca(H_2PO_4)_2 \bullet H_2O$ giving an anorthic crystal structure. The mixture of each shell powder and its produced $Ca(H_2PO_4)_2 \bullet H_2O$ was heated at 900 °C for 3 h, giving rhombohedral crystal β-$Ca_3(PO_4)_2$ powder. FTIR and XRD results of the $CaCO_3$, $Ca(H_2PO_4)_2 \bullet H_2O$, and $Ca_3(PO_4)_2$ prepared from each shell powder are quite similar showing no impurities. Thermal behaviors of $CaCO_3$ and $Ca(H_2PO_4)_2 \bullet H_2O$ produced from each shell are slightly different. Particle sizes and morphologies of all products are significantly different, affected by the kind of shells used. Overall, the bivalve shell wastes were successfully converted to $CaCO_3$, $Ca(H_2PO_4)_2 \bullet H_2O$, and $Ca_3(PO_4)_2$ by a simple, rapid, environmentally benign, and cost-effective approach, which can be a huge potential in many industries providing both economic and ecological benefits according to the Bio-Circular-Green Economy (BCG) model.

Keywords: calcium phosphate; monocalcium phosphate; tricalcium phosphate; calcium carbonate; seashell; bivalve shells

1. Introduction

Seafood productions contribute significantly to the worldwide demand for a protein source, but it also creates a very large quantity of solid and liquid wastes in the processes [1]. For mollusk, over 13 million tons of shell wastes are manufactured annually [2,3]. Three major types of mollusk reported by the Food and Agriculture Organization of the United Nations (FAO) Fisheries and Aquaculture Department are cockle, mussel, and oyster, which are consumed very largely around the world [1]. The main sources are generally from aquaculture rather than wild fisheries, among which oysters are dominant followed by mussels and cockles. In 2018, 5.8, 1.6, and 0.4 million tons of oyster,

Preprints (www.preprints.org) | NOT PEER-REVIEWED | Posted: 1 July 2021 doi:10.20944/preprints202107.0007.v1

mussel, and cockle were produced, respectively [2]. Generally, bivalve shell wastes account for about 65-80% of live weight, which are expected to be over 5 million tons a year [4]. The gigantic numbers of bivalve shells are dumped into public waters and/or landfills, and create many environmental problems including pollution to coastal fisheries, management of public water surface, a unpleasant smell as a consequence of the decomposition of organics attached to the shells, damage of natural landscape, and health/sanitation problems [2-5]. Consequently, the disposal of bivalve shell wastes is becoming an increasingly serious problem for the marine aquaculture industries and various consumer countries. Since the starting of the twenty-first century, there has been an increase in knowledge of sustainable development and research interest in innovative technologies on the conversion of bivalve shell wastes into useful and high-value chemicals and materials [4]. So far, many researchers have studied on characterizations of bivalve (cockles, mussels, and oysters) shells and reported that chemical contents primarily consist of 95-99% aragonite phase of $CaCO_3$ and different organic macromolecules [4]. Based on their environment, the different species of shells may comprise various quantities of oxides such as SiO_2, MgO, Al_2O_3, SrO, P_2O_5, Na_2O, or SO_3 [6-8].

Calcium carbonate ($CaCO_3$) naturally occurs in rocks and shells of various organisms and are widely used in construction, papermaking, pharmaceuticals, agriculture, etc. This compound has three polymorphs in nature, namely, β-$CaCO_3$ (calcite), γ-$CaCO_3$ (aragonite), and μ-$CaCO_3$ (vaterite), in order of increasing stability [6-8]. Currently, the major production of calcium carbonate is from geological sources, which have the risk of heavy metal contamination and are non-renewable resources, unlike calcium carbonate from bio-derived shells which are generally abundant, renewable, inexpensive, and environmentally friendly [1,4]. Based on the above mentioned, recycling seashell wastes to $CaCO_3$ offers many advantages and have potential application in various fields (Figure 1). Various worldwide researches show immense potential for applications of seashells as soil conditioners, catalysts for biodiesel production, adsorbents for removing dyes, toxic metals, radionuclides and phosphates from wastewaters, absorption of SO_2/NO_x and acid gases in flue gas cleaning processes, construction material as a replacement for cement, sand, and coarse aggregate, calcium supplements, calcium animal feed mineral, antibacterial protection, bone implants, etc. [7-9]. However, in Southeast Asia, particularly Thailand, a country with the highest bivalve (cockle, mussel, and oyster) production, the waste shell recycling methods are not developed properly and the shells are mostly dumped as a part of food waste [10,11]. Alarmed with the problems, the Ministry of Higher Education, Science, Research and Innovation of Thailand planned to resolve according to the Bio-Circular-Green Economy (BCG) model and financed a program to set new strategies for recycling these wastes, including establishing factories for producing calcium compounds to increase the recycling quantity of bivalve shell wastes. However, only 30% of bivalve shell wastes are reused/recycled by these factories [12,13].

Preprints (www.preprints.org) | NOT PEER-REVIEWED | Posted: 1 July 2021 doi:10.20944/preprints202107.0007.v1

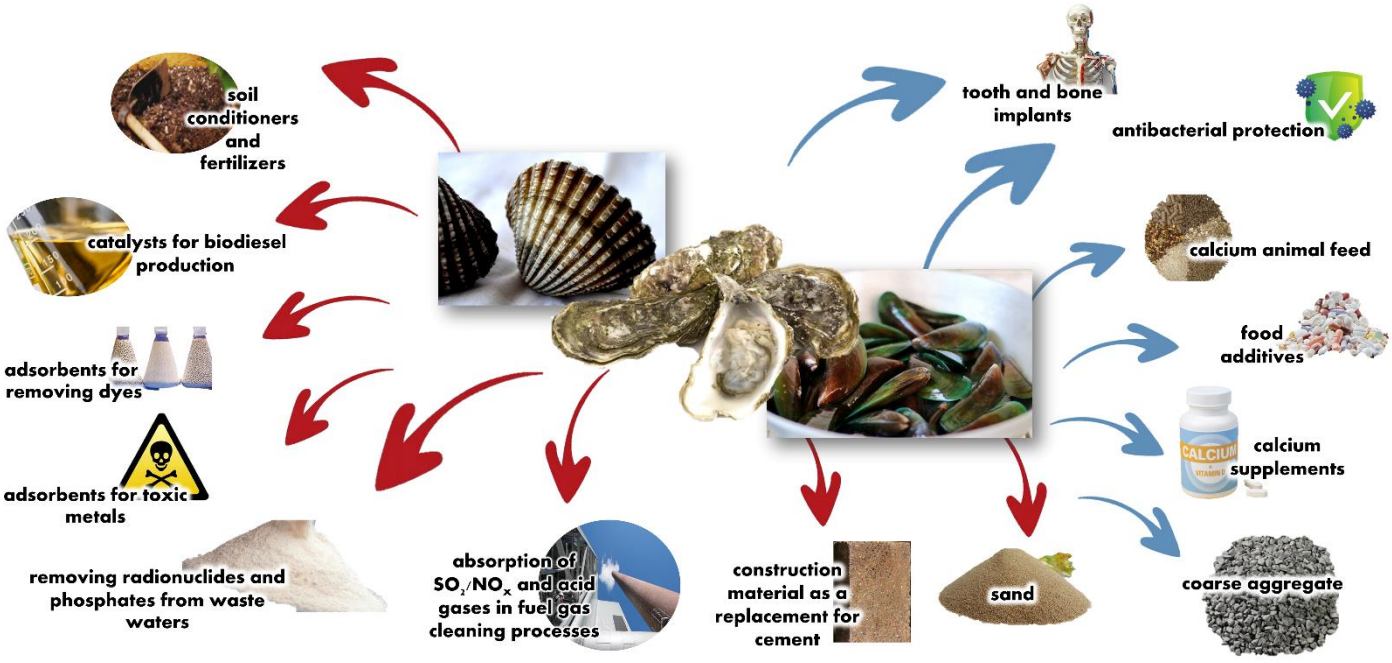

Figure 1. Potential applications of bivalve shell wastes.

Realizing this problem, our research focuses on the conversion of bivalve shells to calcium phosphates, which are used as nutritional supplements, catalysts for some chemical reactions, fertilizers and animal feed minerals, mineral basis of the tooth and bone tissues as well as for creating materials with unique properties [1,4-9]. In Thailand, monocalcium phosphate (MCP) and tricalcium phosphate (TCP) are enormously used in many fields and both compounds are imported every year. MCP has been used in a huge quantity in the agriculture. It is called superphosphate fertilizer, classified by three levels of $\%P_2O_5$ (single (9-20%), double (20-48%), and triple (48-58%) superphosphates), and P-21 for animal feed mineral [12,13]. Additionally, MCP is also used in large amount in the food industry as a buffer, hardener, leavening agent, yeast food, beverage, bakery, and nutrient [14]. TCP is widely used in huge amount in the medical and pharmaceutical industries as medicine, tooth, bone, calcium supplement, in animal feed industry as calcium additive and supplement, and in food industry as acidity regulator, anticaking agent, emulsifier, emulsifying salt, firming agent, flour treatment agent, humectant, raising agent, stabilizer, and thickener in many food substances under the number 341(iii) [15]. Both compounds have been synthesized to produce high-purity grades from various sources of calcium (calcium chloride, calcium carbonate, calcium oxide, calcium nitrate, calcium acetate, etc.) and phosphorus (phosphoric acid, sodium phosphates, potassium phosphates, ammonium phosphates, etc.) by many methods including chemical precipitation [12], hydrothermal synthesis [16,17], microwave assisted methods [18,19], precipitation of emulsions [20], sol-gel [21], crystallization of solutions [22], chemical deposition [23], electrodeposition [24], and mechanic-chemical synthesis [25]. The method used in individual case depends on the desired type of morphology, structure, and chemical content. However, the typical drawback of these synthesized methods is expensive raw materials resulting in high cost of the obtained products which are not suitable to use for some applications such as fertilizer and animal feed industries.

Therefore, one of the solutions for the mention-above issue is to utilize/recycle the bivalve shell wastes in such a way that it can be cost-effectively and resourcefully used to create these calcium phosphates which may resolve some financial problems to purchase costly compounds for many industries in Thailand. Although MCP and TCP have been reportedly prepared from bivalve shell wastes such as oyster shells [26], and Mediterranean mussel shells [27], the methods used complex and high-cost processes which many

Preprints (www.preprints.org) | NOT PEER-REVIEWED | Posted: 1 July 2021 doi:10.20944/preprints202107.0007.v1

parameters must be carefully controlled (concentration, pH, time, and temperature). The aim of this present work is to easily and quickly obtain calcium carbonate from bivalve shell wastes (cockles, mussels, oysters) and then subsequently use it to produce MCP and TCP by using easy, cost-effective, and environmentally benign method. Moreover, this work also highlights some potential applications for shell wastes that can bring both economic and ecological benefits.

2. Materials and Methods

2.1. Starting Reagents

The raw materials used for the current study were waste bivalve shells of cockle, mussel, and oyster collected from seafood restaurants of fishermen residing in areas of Chonburi beaches in eastern Thailand. The individual kind of seashells obtained in the original form was thoroughly cleaned with triply distilled water and dried in an oven at 100 °C for 3 h. Each kind of dried seashell was crushed to produce fine powder by using mortar and pestle and then was sieved in 100 mesh. All fine seashell powders were then characterized to identify the purity and solid phase of calcium carbonate before proceeding to the preparation of the calcium phosphates. Fine seashell powders of cockle, mussel, and oyster were $CaCO_3$ compound and denoted with sample codes CSP, MSP, and OSP, respectively.

2.2. Monocalcium Phosphate Monohydrate ($Ca(H_2PO_4)_2•H_2O$, MCPM) Preparation

A set of monocalcium phosphate hydrate samples was synthesized by the reaction of individual seashell powder (cockle (CSP), mussel (MSP), and oyster (OSP) shells) with 85 wt% phosphoric acid and distilled water, using a constant-addition method modified from previous studies, according to the following generic reaction:

$$CaCO_3(s) + 2H_3PO_4(l) + H_2O(l) \longrightarrow Ca(H_2PO_4)_2•H_2O(s) + CO_2(g) \quad (1)$$

Briefly, 15 mL of 85 wt% H_3PO_4 was slowly added into a beaker (100 mL), which contains 9 g of CSP and was constantly stirred with a Teflon stir bar. This mixing reaction exhibited an exothermic process noticed by increasing temperature (65 °C). Then, 12 mL of distilled water (H_2O) was immediately added into the mixing reaction with constant stirring until CO_2 gas bubbles are no evolved (about 30 min). The resulting reaction was left at room temperature for about 3 h to become dried powder of monocalcium phosphate hydrate without other processes such as filtration and drying with temperature control. The monocalcium phosphate hydrate obtained from CSP was labelled with sample code MCP-C. For MSP and OSP, the processes were repeated in the same way as of CSP and the obtained products were labeled as MCP-M and MCP-O, respectively.

2.3. Tricalcium Phosphate Anhydrous ($Ca_3(PO_4)_2$, TCP) Preparation

A series of tricalcium phosphate samples was prepared by mixing powders of individual seashell powder (cockle (CSP), mussel (MSP), and oyster (OSP) shells) with their prepared monocalcium phosphate hydrate pair (MCP-C, MCP-M, and MCP-O). The generic reaction is:

$$2CaCO_3(s) + Ca(H_2PO_4)_2•H_2O(s) \longrightarrow Ca_3(PO_4)_2(s) + H_2O(g) \quad (2)$$

Typical way, 2.0 g of CSP and 2.52 g of MCP-C were weighed and then well mixing by grinding in a crucible. Then, the mixed powder was heated at 900 °C for 3 h in a furnace. Its final product after heating is tricalcium phosphate, labeled as TCP-C. The tricalcium phosphate powders prepared from the mixed powders of MSP + MCP-M and OSP + MCP-O were prepared in the same way as CSP + MCP-C and the obtained products are labelled as TCP-M and TCP-O, respectively.

2.4. Sample Characterization

Preprints (www.preprints.org) | NOT PEER-REVIEWED | Posted: 1 July 2021 doi:10.20944/preprints202107.0007.v1

2.4.1 Thermogravimetric Analysis (TA)

The thermal behaviors of the dried fine seashell powders and monocalcium phosphate monohydrate were analyzed by a thermogravimetric/differential thermal analyzer (TG-DTA, Pyris Diamond, Perkin Elmer). The experiments were performed in static air, at the heating rates of 10 °C min^{-1} over the temperature range from 30 to 900 °C and the O_2 flow rate of 100 mL min^{-1}. The sample mass of about 6.0-10.0 mg was filled into alumina crucible without pressing. The thermogram of a sample was recorded in an open aluminium pan using Al_2O_3 as the reference material.

2.4.2. Fourier Transform Infrared (FT-IR) Spectroscopy

The molecular structures were measured by a Fourier Transform Infrared Spectrophotometer (FT-IR, Spectrum GX, Perkin Elmer), which were recorded in the range of 4000-400 cm^{-1} with eight scans and the resolution of 4 cm^{-1} using KBr pellets (spectroscopy grade, Merck).

2.4.3. Powder X-ray Diffraction

The crystal phase of the obtained samples was detected by powder X-ray diffraction (XRD) analysis. The specimen was ground into a fine powder and used for the analysis. XRD patterns were recorded with an X-ray diffractometer (D8 Advance, Bruker AXS GmbH) using monochromatized X-ray (CuKα: λ = 0.1542 nm) operating at the condition of 40 kV and 40 mA. The diffraction angle was continuously scanned from 10° to 60° in 2θ at a scanning rate of 2°/min. A range of 10°-60° is shown in the figures because no relevant peaks were observed in the excluded region.

2.4.4. Scanning Electron Microscopy

Samples were dried, mounted with carbon tape, and secondary electron images were taken (Phenom PRO, Pheonom-World, Eindhoven, The Netherlands) at magnifications of 165×, 500×, and 1000×. The images were scanned at 10 kV and a resolution of 2048 dpi, with an exposure time of 26 s.

3. Results and Discussion

3.1. Characterization Results of Bivalve Shell Powders

Bivalve shell powders including cockle (CSP), mussel (MSP), and oyster (OSP) contain a calcium carbonate content of about 98% in each sample as determined by XRD. Figure 2 displays TG/DTG curves of the CSP, MSP, and OSP samples, which are quite similar. TG lines of each sample show the mass loss in the range of 600-800 °C, which correspond to a strong single peak of DTG curves at 752, 772, 750 °C for the CSP, MSP and OSP samples, respectively. The quantities of mass loss (remaining mass) are found to be 43.06 % (56.94 %) for the CSP and 43.88 % (56.12 %) OSP samples and 48.40 % (51.60 %) for the MSP sample. The thermal results were well consistent with those of the reference data of $CaCO_3$ and theoretical data [28-30]. The thermal behavior obtained indicates that the bivalve shell powders can be transformed to CaO by calcination at above 772 °C, which may be useful for the production of this compound to be used in specific applications.

Preprints (www.preprints.org) | NOT PEER-REVIEWED | Posted: 1 July 2021 doi:10.20944/preprints202107.0007.v1

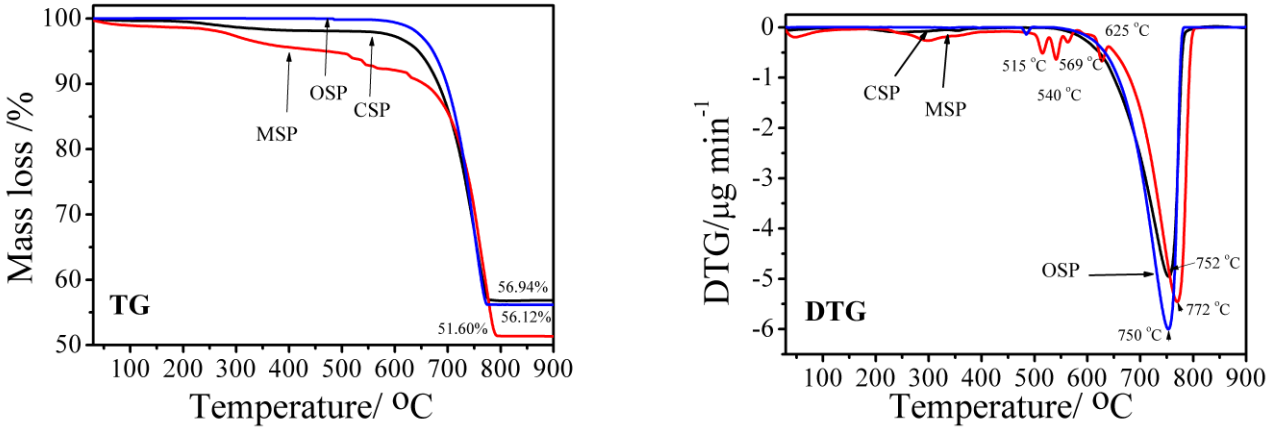

Figure 2. TG and DTG curves of the bivalve shell (CSP, MSP and OSP) powders.

Figure 3 illustrates FTIR spectra of the CSP, MSP, and OSP samples that are quite similar due to fundamental vibrational bands of CO_3^{2-} block unit in the $CaCO_3$ structure for each sample. The vibrational modes of CO_3^{2-} anion are divided into three types [31]: (i) vibrations of (CO_3^{2-}) groups (internal modes), (ii) vibrations of hydroxyl molecule (in the case of hydroxyl carbonates ≈ 900 cm^{-1}, 1500-1600 cm^{-1} and 3400 cm^{-1}), and (iii) vibration modes M-O from the interactions between the cation and oxygen of either (CO_3^{2-}) or OH^- (external or lattice modes). The carbonate anion (CO_3^{2-}) is a nonlinear four-atomic species and it must have 3(4)-6=6 normal modes of vibrations [32]. The six normal vibrational modes are nondegenerate symmetric stretch (v_1; A'1: Raman active), nondegenerate asymmetric (out of plane) bend (v_2; A"1: IR active), doubly degenerate asymmetric stretch (v_3; E': Raman and IR active), doubly degenerate symmetric (in-plane) bend (v_4; E': Raman and IR active). FTIR spectra of the CSP, MSP, and OSP samples were analyzed according to this theory. Two strong intense bands at 696 cm^{-1} and 863 cm^{-1} are assigned to the v_4 and v_2 modes, respectively. A weak band at 1030 cm^{-1} is contributed to v_1 mode. A band at 1413 cm^{-1} looking like a mountain is related to v_3 mode. A weak band observed at 1782 cm^{-1} may be regarded as the combination bands of $v_4 + v_1$ modes. A weak band at 2520 cm^{-1} and a broad band around 2875 cm^{-1} may be regarded as combination of or/and overtone of v_4, v_3, and v_1 modes. A single band of the OH-stretching modes is observed at 3453 cm^{-1}. For FTIR results of all bivalve shells, the v_1 mode that appear normally active in Raman is observed and v_3 and v_4 modes are not shown doubly degenerate bands, which may be correlated with the atomic masses of the cations and the presence of the molecules belonging to site symmetry of their structures [33]. The FTIR results obtained are very similar to that of the calcite phase of $CaCO_3$ in literature [32,33], which indicates that the CSP, MSP, and OSP samples have main content as this crystalline phase.

X-ray diffraction patterns of the CSP, MSP and OSP samples are very similar and shown in Figure 4. Bivalve (cockle, mussel, and oyster) shells are biological wastes, which are mainly made up of calcium carbonate (≥ 96 wt%) and minor contaminations of other minerals. It can clearly be seen that the major crystalline phases of the CSP, MSP, and OSP samples are calcite (β-$CaCO_3$). No peaks due to other phases were observed, confirming the high purity of raw material under study. The diffraction intensity is the calcite (002) 2θ = 29.81 and the next to strongest are the calcites at (111), (012), (202), (112) (200) and (202), respectively. The XRD analysis revealed that the crystalline form of calcium carbonate in the CSP, MSP, and OSP samples was calcitic polycrystals, which was found to match with the PDF data file of $CaCO_3$ (File no.72-1937) [30,34]. The XRD results are well agreement with the FTIR data.

Preprints (www.preprints.org) | NOT PEER-REVIEWED | Posted: 1 July 2021 doi:10.20944/preprints202107.0007.v1

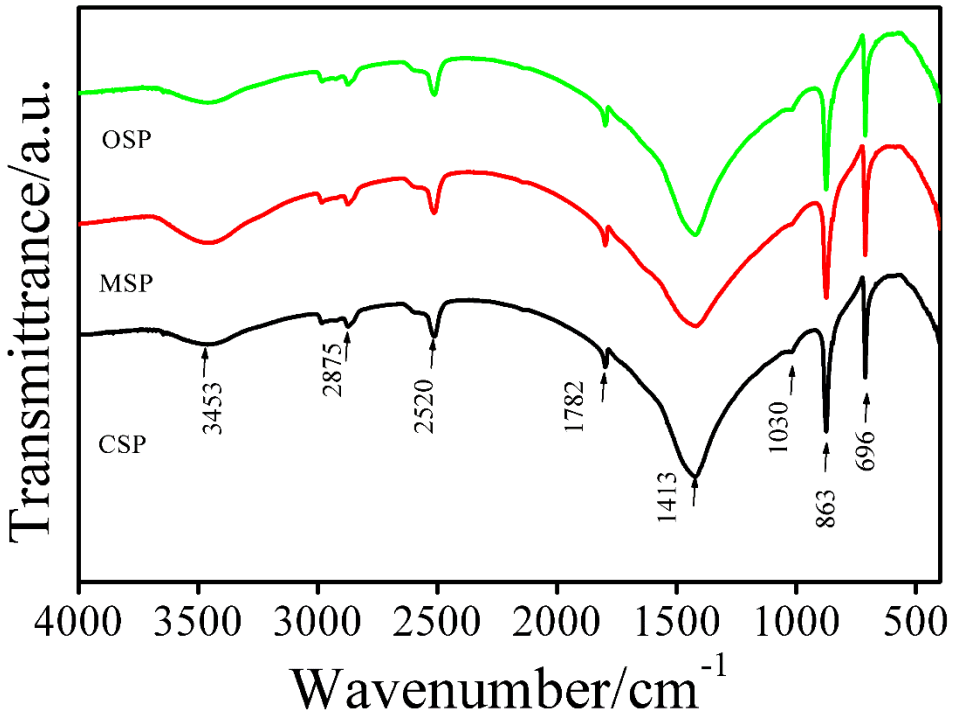

Figure 3. FTIR spectra of the bivalve shell (CSP, MSP and OSP) powders.

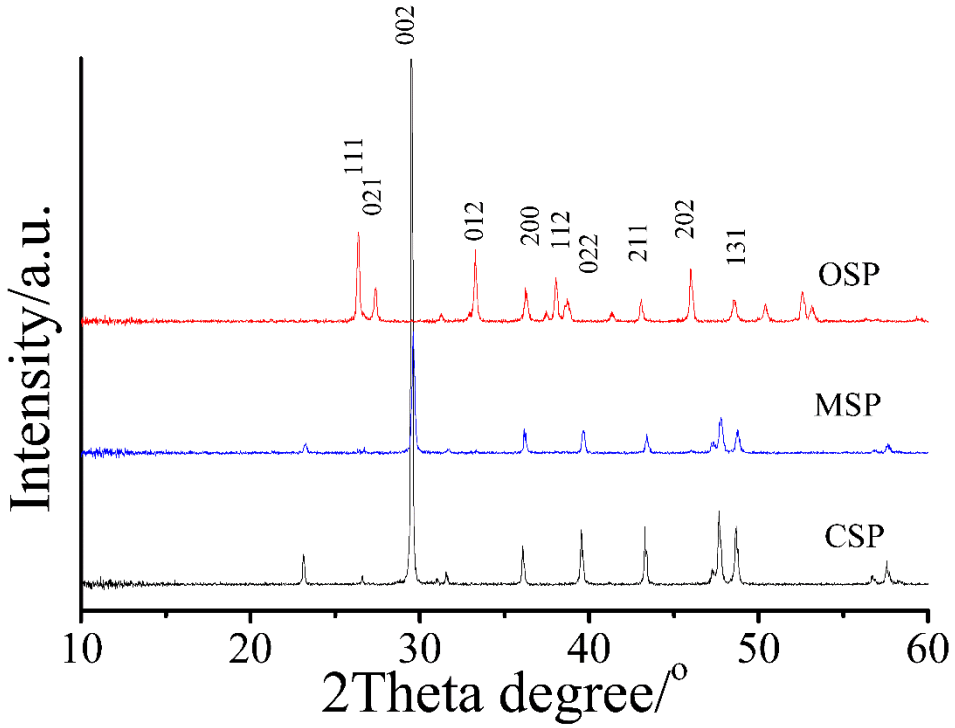

Figure 4. XRD patterns of the bivalve shell (CSP, MSP and OSP) powders.

SEM micrographs of the CSP, MSP and OSP samples exhibit different morphological features and are shown in Figure 5. SEM image of CSP reveals elongated, partly polyhedral rod-like crystals (up to 10 μm long) with different sizes and forms. SEM image of MSP reveals elongated, partly polyhedral sheet wood-like crystals with different sizes, which are randomly placed horizontally and vertically. Finally, SEM image of OSP reveals needle-like crystals of different sizes, which are agglomerated.

Preprints (www.preprints.org) | NOT PEER-REVIEWED | Posted: 1 July 2021 doi:10.20944/preprints202107.0007.v1

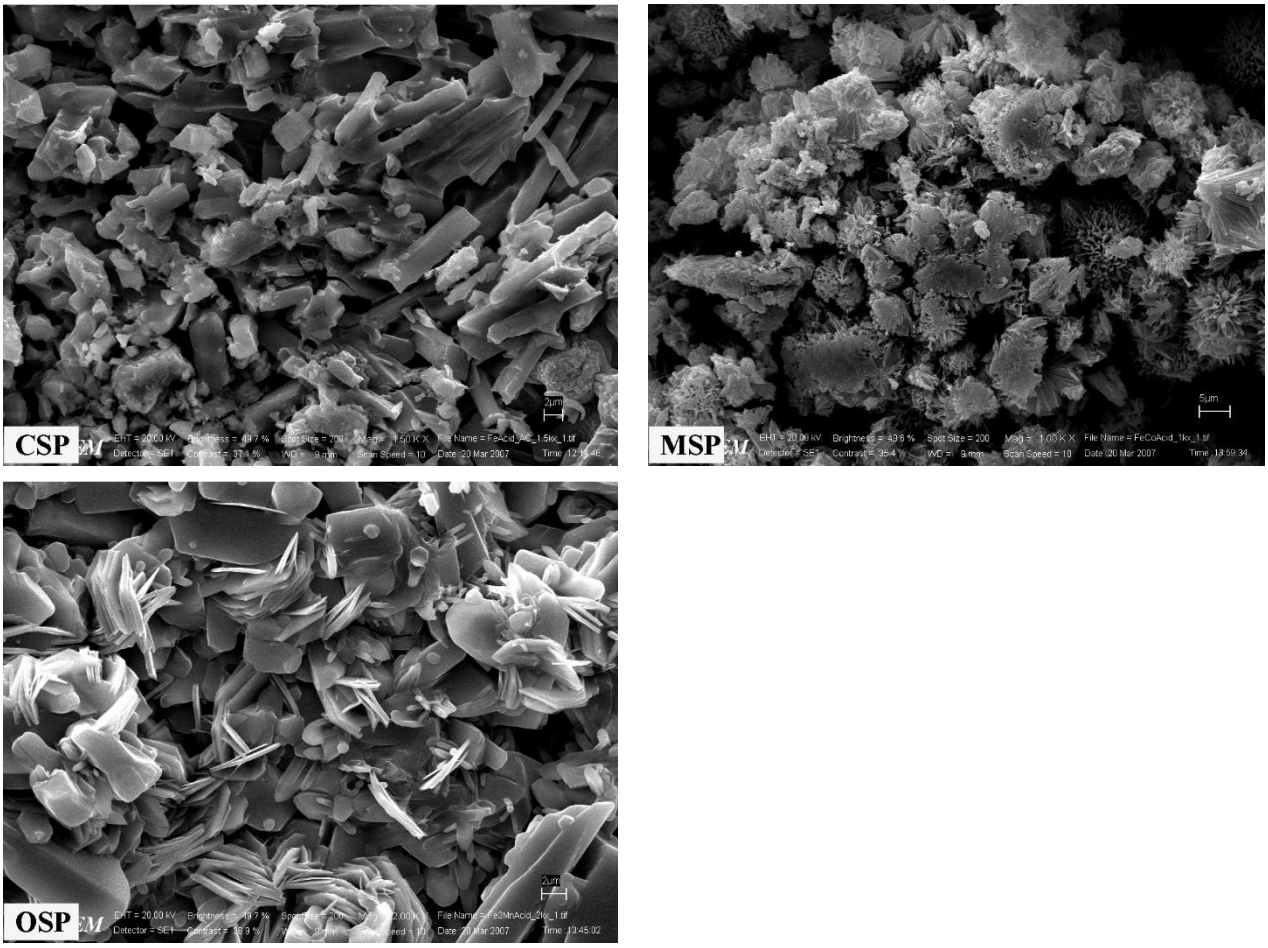

Figure 5. SEM micrographs of the bivalve shell (CSP, MSP and OSP) powders.

3.2. Characterization Results of Monocalcium Phosphates

TG/DTG curves of three monocalcium phosphate samples prepared from cockle (CSP), mussel (MSP), and oyster (OSP) shell powders, labeled as MCP-C, MCP-M, and MCP-O, respectively, are displayed in Figure 6. TG lines of all samples showing the mass loss in the range of 100-600 °C are similar. The mass remains occurred at above 600 °C, which are found to be 81.08, 75.00, and 82.70 % for MCP-C, MCP-M, and MCP-O, respectively. The mass losses found to be around 20 % for each sample are related to the loss of three water molecules in structure. The mass loss and mass remain of each sample are close to that of theoretical values at 21 and 79 %, respectively [30,35]. The relative with TG data, DTG curves of the MCP-C, MCP-M, and MCP-O samples showing the numbers and peak positions of steps of thermal transformation are different. Four DTG peaks are observed at 127, 178, 224, and 330 °C for the CSP sample and 127, 185, 245, and 330 °C for the MSP sample while five DTG peaks occur at 127, 185, 224, 265, and 330 °C for the OSP sample. Two peaks occurred below 200 °C correspond to the dehydration steps of about one molecule of water crystal. Two/three peaks observed in the range of 200-330 °C relate to deprotonated steps of two dihydrogen phosphate ($H_2PO_4^-$) anions. General mechanism reactions of thermal transformation could be:

$$Ca(H_2PO_4)_2 \bullet H_2O(s) \xrightarrow{\text{below 200 °C}} Ca(H_2PO_4)_2(s) + H_2O(g) \quad (3)$$

$$Ca(H_2PO_4)_2(s) \xrightarrow{\text{200-330 °C}} Ca_3(PO_3)_2(s) + 2H_2O(g) \quad (4)$$

Preprints (www.preprints.org) | NOT PEER-REVIEWED | Posted: 1 July 2021 doi:10.20944/preprints202107.0007.v1

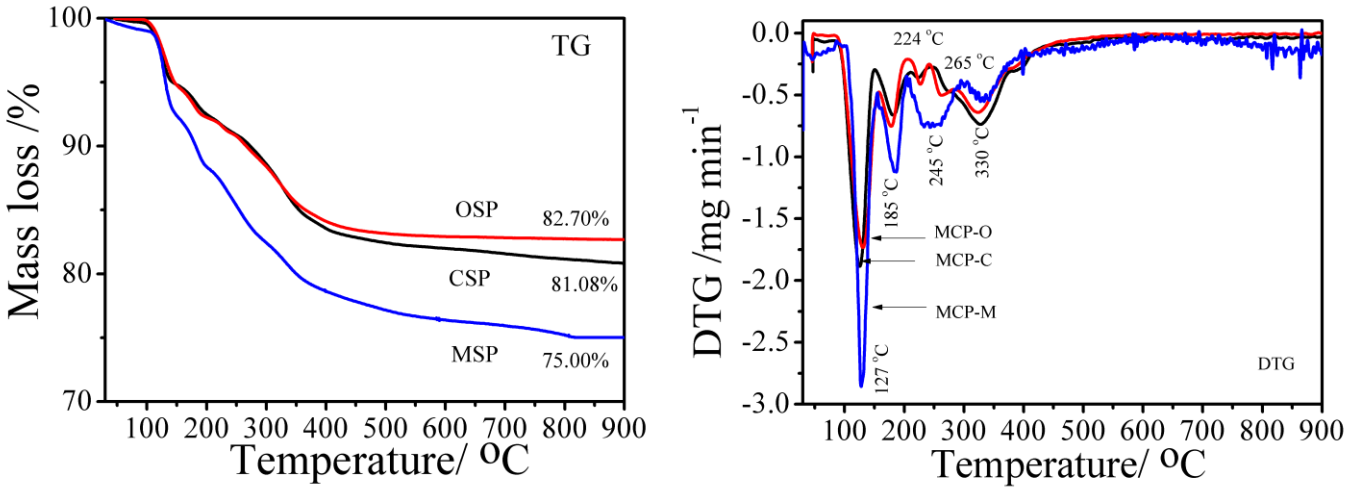

Figure 6. TG and DTG curves of MCP-C, MCP-M and MCP-O samples.

For $Ca(H_2PO_4)_2 \bullet H_2O$ prepared from bivalve shells, reaction (4) of its transformation to polyphosphate $Ca_3(PO_3)_2$ occurs at above 400 °C. Reactions (3) and (4) observed more than one mechanism according to many peaks in DTG curves indicate different inter/intramolecular interactions due to the different surroundings of water and $H_2PO_4^-$ within the structure. Thermal behavior of $Ca(H_2PO_4)_2 \bullet H_2O$ prepared from different bivalve shells giving the different results indicate clearly that this property dependent on raw materials.

Figure 7 presents FTIR spectra of the MCP-C, MCP-M, and MCP-O samples that are very similar because of fundamental vibrational bands of $H_2PO_4^-$ and H_2O block units in the $Ca(H_2PO_4)_2 \bullet H_2O$ structure for each sample. The vibrational modes of $H_2PO_4^-$ anion are characterized by two types [36,37]: (i) the PO_4^{3-} (T_d symmetry) internal vibrations, and (ii) the vibrations involving OH motions. The dihydrogen phosphate anion ($H_2PO_4^-$) is a nonlinear seven-atomic species and it must have 3(7)-6=15 normal modes of vibrations [32]. The nine vibrations coming from the PO_4^{3-} (T_d symmetry) contain well-known normal modes: $\nu_1(A_1)$ and $\nu_3(F_2)$ are symmetric and asymmetric stretching modes, respectively; $\nu_2(E)$ and $\nu_4(F_2)$ are symmetric and asymmetric bending modes, respectively. The existence of two P-OH bonds results in a reduction a reduction of the molecular symmetry of $H_2PO_4^-$ and its highest possible symmetry is C_{2v}. As a result, the degenerate modes of $\nu_2(E)$, $\nu_3(F_2)$ and $\nu_4(F_2)$ are fully lifted: $\nu_2(E)$ splits into two components (A_1+A_2) and $\nu_3(F_2)$ and $\nu_4(F_2)$ into three components (A_1+B_1+B_2) each. These eight vibrations happen from the intra-ionic coupling for the PO_4 stretching vibrations (two longer P- OH and two shorter P-O bonds), which may also be regarded as $\nu_s(P(OH)_2)$, $\nu_{as}(P(OH)_2)$, $\nu_s(PO_2)$, and $\nu_{as}(PO_2)$ for each $H_2PO_4^-$ group. The six vibrations linking OH motions are characteristic for $H_2PO_4^-$: ν(OH), δ(OH), and γ(OH) for each POH group (i.e., OH stretching, POH in-plane and out-of-plane bending vibrations, respectively). For water molecule, fundamental vibrations contain three normal vibrations: symmetric stretching (ν_1(OH)), symmetric bending(ν_2(HOH)), and asymmetric stretching (ν_3(OH)) and three vibrations (wagging, rocking, and twisting). The bands observed in spectra of each sample are 493, 565, 690, 862, 963, 1091, 1164, 1237, 1388, 1679, 1700, 2311, 2440, 2963, 3263, 3470 cm^{-1}, which are assigned to $\nu_2(PO_4^{3-})$, $\nu_4(PO_4^{3-})$, $L_1(H_2O)$, γ(OH), $\nu_{as}(P(OH)_2)$, $\nu_s(PO_2)$, $\nu_{as}(PO_2)$, δ(OH)(1), δ(OH)(2), ν_2(HOH), ν(OH) or band C, ν(OH) or band B, ν(OH) or band B, ν(OH) or band A, (ν_1(OH)) of H_2O, and (ν_3(OH)) of H_2O, respectively [38]. The FTIR results obtained are very similar to that of the $Ca(H_2PO_4)_2 \bullet H_2O$ in literature [38], which confirms that the MCP-C, MCP-M, and MCP-O samples have major content as this crystal phase.

Preprints (www.preprints.org) | NOT PEER-REVIEWED | Posted: 1 July 2021 doi:10.20944/preprints202107.0007.v1

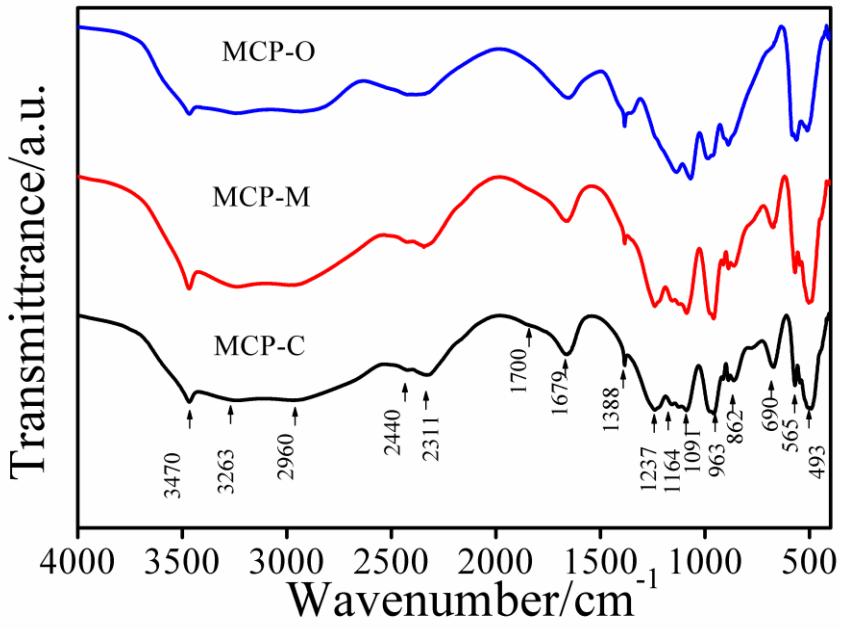

Figure 7. FTIR spectra of MCP-C, MCP-M and MCP-O samples.

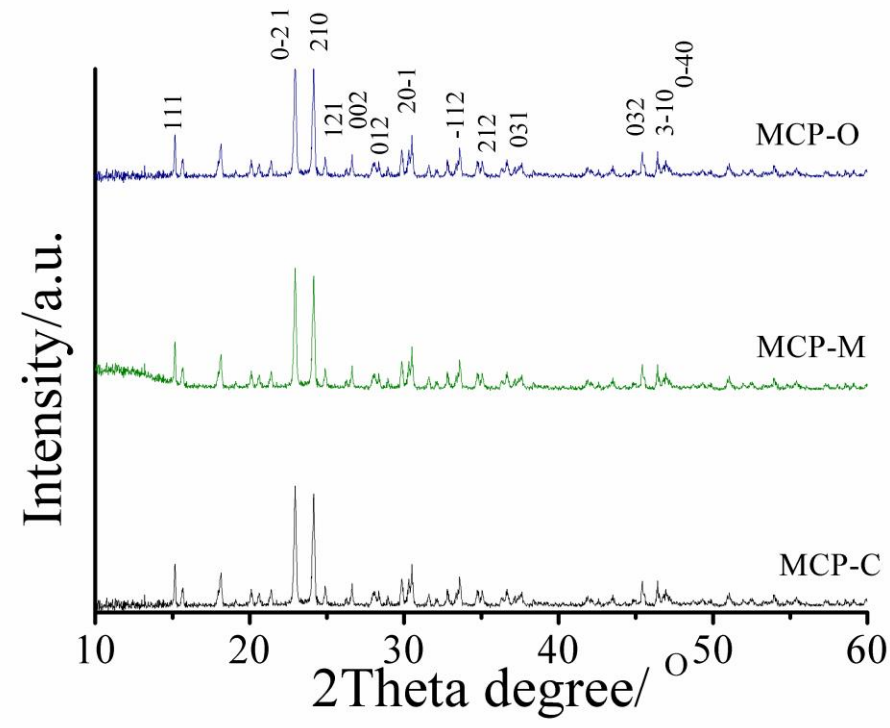

Figure 8. XRD patterns of MCP-C, MCP-M and MCP-O samples.

X-ray diffraction patterns of the MCP-C, MCP-M, and MCP-O samples (Figure 8) are the same 2θ positions but intense peaks are different. All detectable peaks of the obtained MCP-C, MCP-M, and MCP-O samples are indexed as $Ca(H_2PO_4)_2 \bullet H_2O$ structure, which are identified using the standard data of PDF# 700090 [30,35]. XRD patterns exhibits two sharp characteristic peaks at 2θ = 22.95 and 24.18° corresponding to (0-21) and (210) reflections for anorthic crystal structure with space group Pî of $Ca(H_2PO_4)_2 \bullet H_2O$. The labeled diffraction peaks can be indexed according to standard XRD data and no peaks due

Preprints (www.preprints.org) | NOT PEER-REVIEWED | Posted: 1 July 2021 doi:10.20944/preprints202107.0007.v1

to other phases were observed, confirming the high purity of obtained compounds under study. The XRD results and the FTIR data are well coincident.

Figure 9 presents the typical micrographs of the three selected powder (MCP-C, MCP-M, and MCP-O) samples. As shown in Figure 9, the MCP-C particles look petal-like with roughness surface and highly agglomerated. The MCP-M particles seem to have inherited the polyhedral of the plate-like microstructures with smooth surfaces. The MCP-O particles show smooth surfaces of polyhedral wood sheet-like morphologies in the horizontal direction. Particle sizes and morphologies of three $Ca(H_2PO_4)_2 \bullet H_2O$ samples prepared different bivalve (cockle, mussel and oyster) shells are slightly different and significantly different from those of raw material powders; calcium carbonate obtained from cockle, mussel and oyster shells.

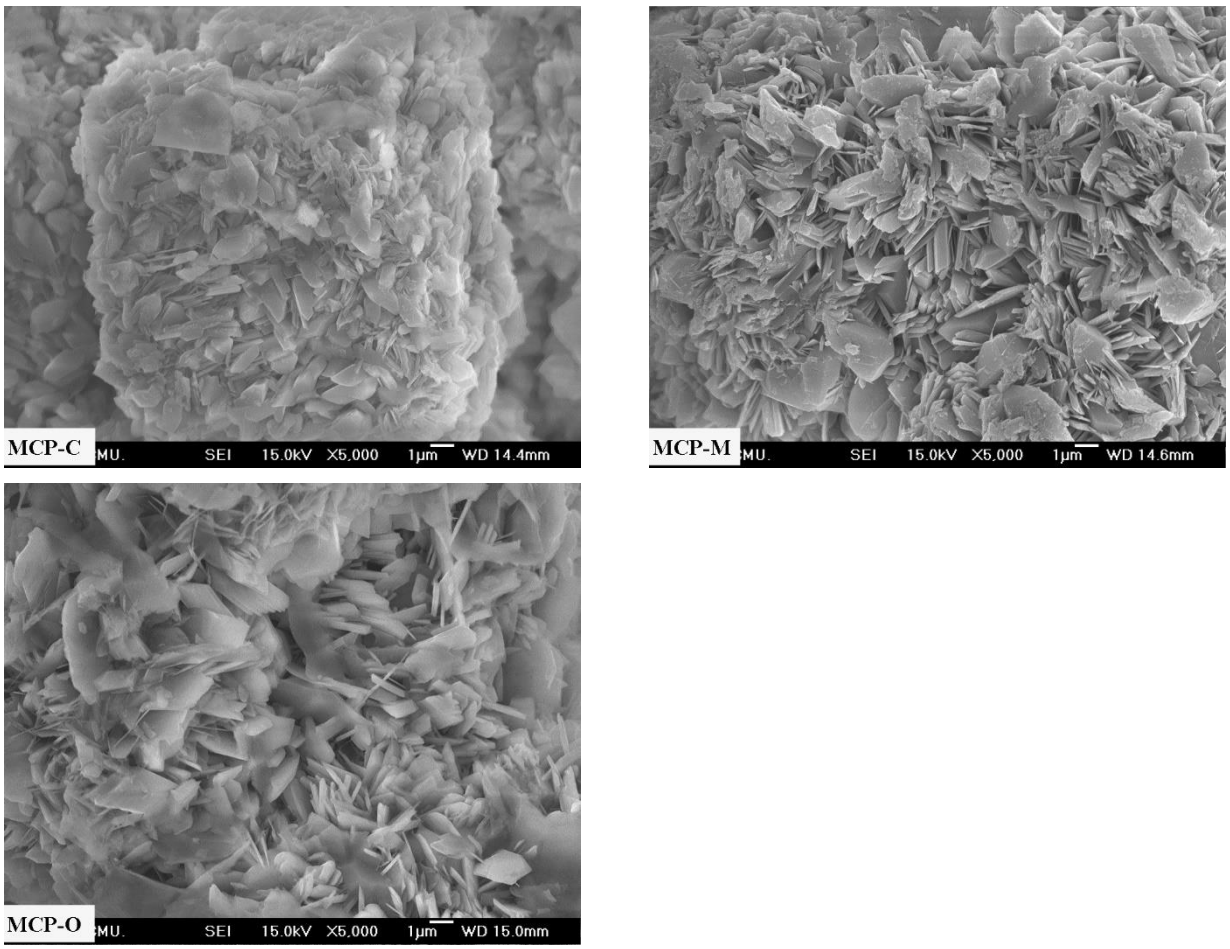

Figure 9. SEM micrographs of MCP-C, MCP-M and MCP-O samples.

3.3. Characterization Results of Tricalcium Phosphates

For FTIR spectra of tricalcium phosphates prepared from the calcination of the mixture of the produced monocalcium phosphates with its calcium raw materials (cockle, mussel, and oyster shells), labeled as the TCP-C, TCP-M, and TCP-O and shown in Figure 10. The FTIR spectra of each sample are very similar due to the fundamental vibrating unit, PO_4^{3-} anion containing within the structure. Vibration bands of $PO_4^{3-}(T_d)$ are well-known as four characteristic modes, which consist of symmetric stretching ($\nu_1(A_1)$; singly degeneracy), asymmetric stretching ($\nu_3(F_2)$; triply degeneracy), symmetric bending vibrations ($\nu_2(E)$; doubly degeneracy), and asymmetric bending ($\nu_4(F_2)$; triply degeneracy) vibrations and it must have 3(5)-6=9 normal modes of vibrations for each group,

Preprints (www.preprints.org) | NOT PEER-REVIEWED | Posted: 1 July 2021 doi:10.20944/preprints202107.0007.v1

discussed similarly with the previous section [30]. In theory, the $\nu_3(F_2)$ and $\nu_4(F_2)$ modes are active in infrared while the $\nu_1(A_1)$ and $\nu_2(E)$ modes are active in Raman [31]. Vibrational bands of PO_4^{3-} anion for all prepared products detected in the regions of 700-450 and 1250-900 cm^{-1} are defined to the $\nu_4(PO_4^{3-})$ and $\nu_3(PO_4^{3-})$ modes, respectively. Various peaks in these spectral regions verify the being of distinct nonequivalent phosphate units in each structure and the loss of the degenerate vibrational modes affecting correlation field splitting [31,32]. Additionally, the observation of a strong ν_s(POP) bands (721 cm^{-1}) is known to be the most striking feature of polyphosphate spectrum.

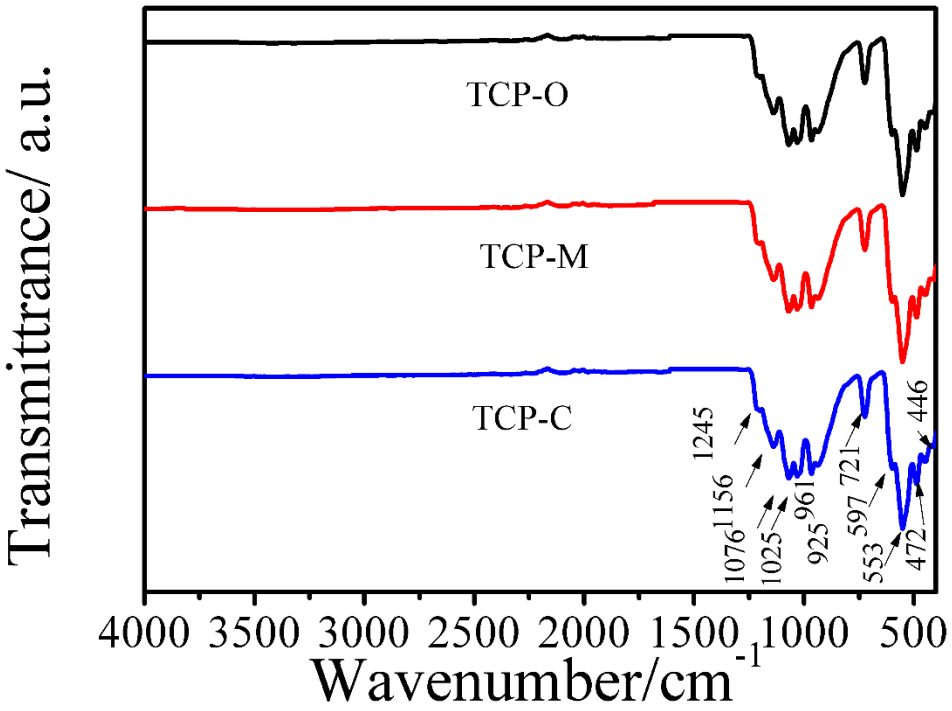

Figure 10. FTIR spectra of TCP-C, TCP-M and TCP-O samples.

The XRD patterns of TCP-C, TCP-M, and TCP-O samples were indexed using standard cards by the Joint Committee on Powder Diffraction and Standards (JCPDS), exhibited in Figure 11. The powders performed by different shells matched with the card number 00-055-0898. In all the samples, the maximum peak corresponding to the crystallinity of beta phase was found at $2\theta = 31.5°$, corresponding to the (021) planes, and indicating rhombohedral crystal structure with space group R3c, which agrees with the previous reports [39,40]. From the XRD data of the prepared TCP samples, no other characteristic peaks related to impurities and any intermediate or remaining raw materials are observed, which further confirm that the synthesized products are pure β-$Ca_3(PO_4)_2$ powders. The FTIR results of all the synthesized samples obtained are consistent with the XRD data, which confirm the identification of each compound.

Preprints (www.preprints.org) | NOT PEER-REVIEWED | Posted: 1 July 2021 doi:10.20944/preprints202107.0007.v1

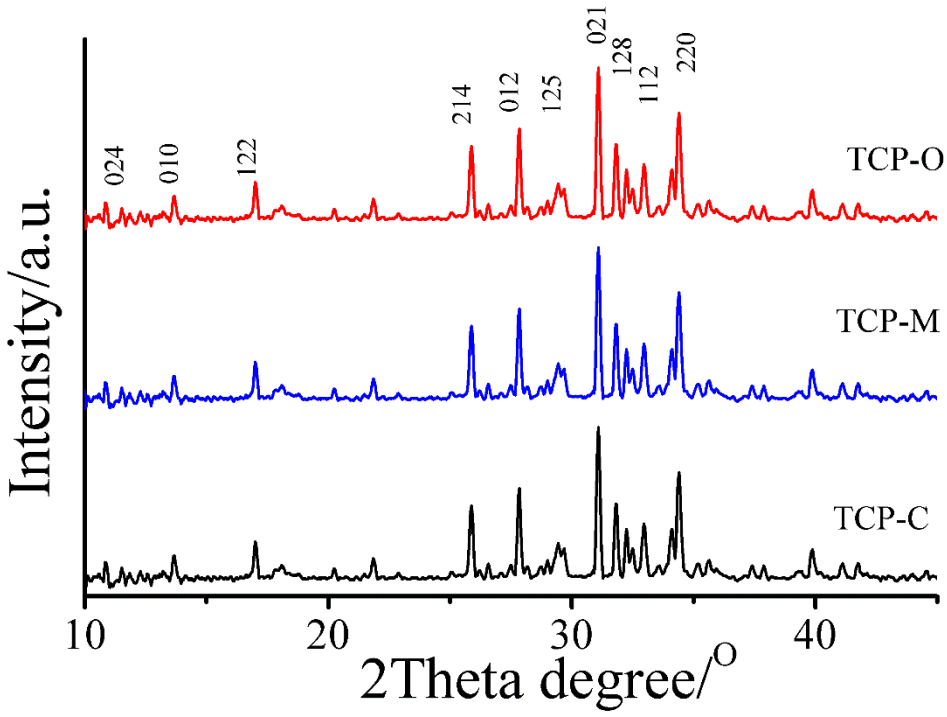

Figure 11. XRD patterns of TCP-C, TCP-M and TCP-O samples.

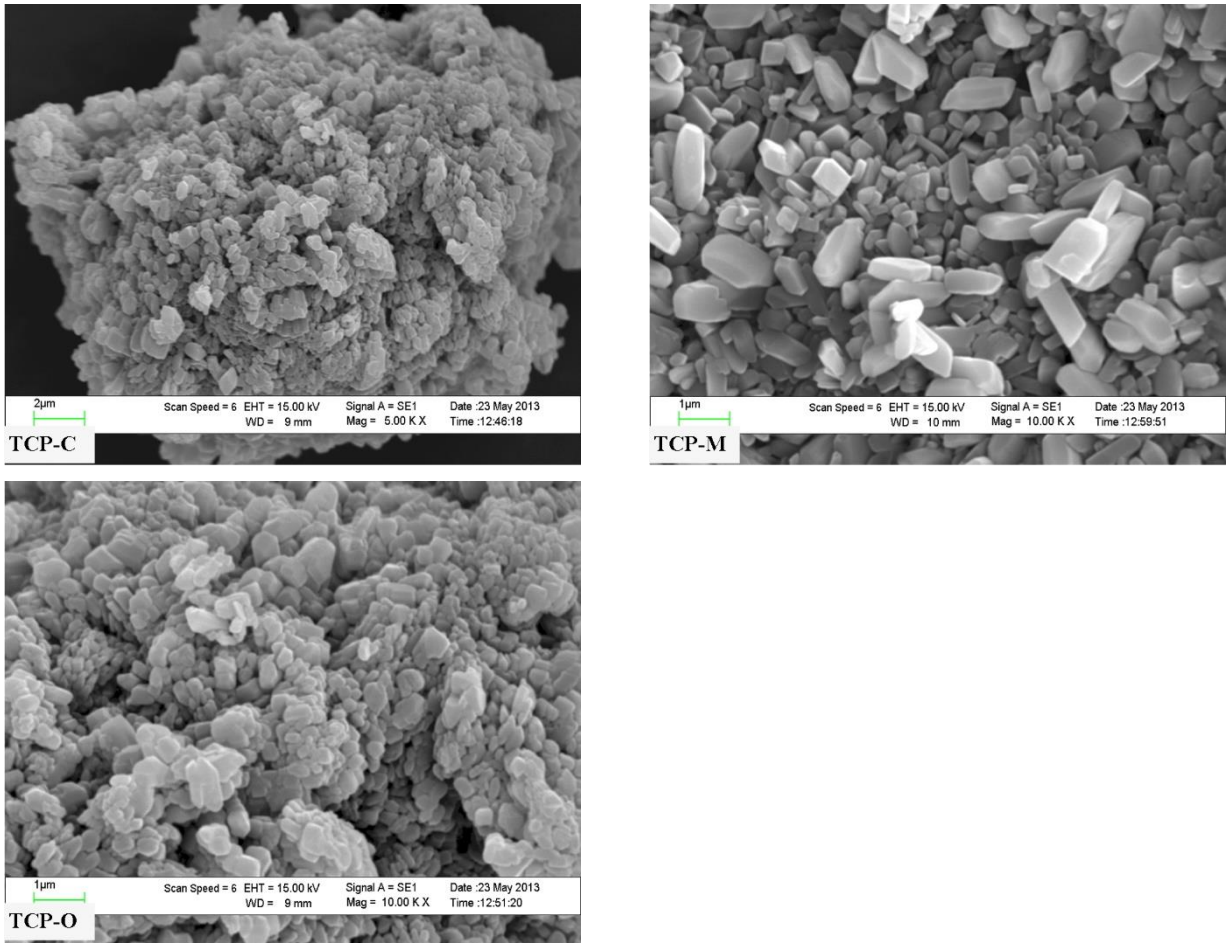

Figure 12. SEM micrographs of TCP-C, TCP-M and TCP-O samples.

 doi:10.20944/preprints202107.0007.v1

The typical micrographs of the three selected powder (TCP-C, TCP-M, and TCP-O) samples are presented in Figure 12. The TCP-C particles look like the coarse surface on polyhedral spherical and highly agglomerated. The TCP-M particles that were like rice grain-type granular with uniform particles of 2.0-5.0 μm in size and agglomerations appear. The TCP-O particles were like polyhedral granular with identical particles of 2.0-5.0 μm in size and smooth surfaces. The difference of particle sizes and morphologies of three $Ca_3(PO_4)_2$ samples are caused by the different kinds of used bivalve shells as raw reagents. The SEM micrograph data of the obtained products are significantly different from those of raw material powders; calcium carbonate and monocalcium phosphate prepared from cockle, mussel, and oyster shells.

4. Conclusions

To recover the bivalve shell wastes for potential use, scientists, researchers, technologists, and industrialists need to be aware of the properties of these materials, how they can be applied, and what limitations may be related to their use. The main purpose of this work was to convert bivalve (cockle, mussel and oyster) shell wastes to advanced calcium compounds as calcium carbonate, monocalcium phosphate and tricalcium phosphate. Natural calcium carbonate powders with calcite crystal phase were easy to obtain by gridding bivalve (cockle, mussel and oyster) shell wastes. Each bivalve shell powder was reacted with 85 wt% phosphoric acid and water to prepare monocalcium phosphate by a new special procedure that is a simple, rapid, cost-effective, and environmentally friendly method. The calcination of the mixture of each bivalve shell powder with its produced monocalcium phosphate at 900 °C for 3 h got β-tricalcium phosphate powder. Calcium carbonates, monocalcium phosphate, and tricalcium phosphates prepared from various (cockle, mussel, and oyster) shell powders gave FTIR and XRD results of each kind of compounds that were much resembled and well consistent with previous reports, which demonstrated no apparent impurities indicating high purities of the all the obtained products. The slight differences in thermal properties of the calcium carbonates and monocalcium phosphates prepared depend on starting shell powders. The morphologies of all the prepared samples are significantly different clearly indicating raw material's effect on this property. Overall, in this work, calcium carbonate, monocalcium phosphate and tricalcium phosphates converted from these bivalve shell wastes were a huge potential to use in many industrials bringing about both environmental and economic benefits.

Author Contributions: S.S. conceived and designed the experiments; B.B. performed the experiments, analyzed the data and wrote the manuscript; K.C. contributed SEM observations and proved the manuscript; and W.B. and N.L. discussed the experiments and the manuscript.

Funding: This research was funded by the Thailand Science Research and Innovation (TSRI), grant number RE-KRIS/008/64.

Institutional Review Board Statement: Not applicable.

Informed Consent Statement: Not applicable.

Data Availability Statement: The data presented in this study are available on request from the corresponding author.

Acknowledgments: The authors would like to thanks the Scientific Instruments Center KMITL for supporting TGA, FTIR, XRD, and SEM techniques.

Conflicts of Interest: The authors declare no conflict of interest.

 doi:10.20944/preprints202107.0007.v1

References

1. Yang, H.; Yan, N. Transformation of Seafood Wastes into Chemicals and Materials. *Encyclopedia of Sustainability Science and Technology* **2012**.
2. FAO. *The State of World Fisheries and Aquaculture 2020. Sustainability in action*; Rome, 2020.
3. Yan, N.; Chen, X. Sustainability: Don't waste seafood waste. *Nature* **2015**, *524*, 155-157.
4. Miculescu, F.; Mocanu, A.-C.; Maidaniuc, A.; Dascălu, C.-A.; Miculescu, M.; Voicu, Ș.I.; Ciocoiu, R.-C. Biomimetic Calcium Phosphates Derived from Marine and Land Bioresources. *Hydroxyapatite - Advances in Composite Nanomaterials, Biomedical Applications and Its Technological Facets* **2018**.
5. Vecchio, K.S.; Zhang, X.; Massie, J.B.; Wang, M.; Kim, C.W. Conversion of bulk seashells to biocompatible hydroxyapatite for bone implants. *Acta Biomater.* **2007**, *3*, 910-918.
6. Zhang, X.; Vecchio, K.S. Conversion of natural marine skeletons as scaffolds for bone tissue engineering. *Front. Mater. Sci.* **2013**, *7*, 103-117.
7. Wu, S.-C.; Hsu, H.-C.; Wu, Y.-N.; Ho, W.-F. Hydroxyapatite synthesized from oyster shell powders by ball milling and heat treatment. *Mater. Charact.* **2011**, *62*, 1180-1187.
8. Shavandi, A.; Bekhit, A.E.-D.A.; Ali, A.; Sun, Z. Synthesis of nano-hydroxyapatite (nHA) from waste mussel shells using a rapid microwave method. *Mater. Chem. Phys.* **2015**, *149-150*, 607-616.
9. Bhattacharjee, B.N.; Mishra, V.K.; Rai, S.B.; Parkash, O.; Kumar, D. Structure of apatite nanoparticles derived from marine animal (crab) shells: An environment-friendly and cost-effective novel approach to recycle seafood waste. *ACS Omega* **2019**, *4*, 12753-12758.
10. FAO. *The State of World Fisheries and Aquaculture 2018 - Meeting the sustainable development goals*; Rome, 2018.
11. Jovic, M.; Mandic, M.; Sljivic-Ivanovic, M.; Smiciklas, I. Recent trends in application of shell waste from mariculture. *Stud. Mar.* **2019**, *32*, 47-62.
12. Seesanong, S.; Laosinwattana, C.; Chaiseeda, K.; Boonchom, B. A simple and rapid transformation of golden apple snail (*Pomacea canaliculata*) shells to calcium carbonate, monocalcium and tricalcium phosphates. *Asian J. Chem.* **2019**, *31*, 2522-2526.
13. Seesanong, S.; Laosinwattana, C.; Boonchom, B. Microparticles of calcium carbonate $CaCO_3$, calcium hydrogen phosphate hydrate $CaHPO_4{\cdot}1.9H_2O$ and tricalcium phosphate $Ca_3(PO_4)_2$ prepared from golden apple snail shells (*Pomacea canaliculata*). *Res. J. Chem. Environ.* **2020**, *24*, 1-6.
14. Sánchez-Enríquez, J.; Reyes-Gasga, J. Obtaining $Ca(H_2PO_4)_2{\cdot}H_2O$, monocalcium phosphate monohydrate, via monetite from brushite by using sonication. *Ultrason. Sonochem.* **2013**, *20*, 948-954.
15. Dorozhkin, S.V. Biphasic, Triphasic, and Multiphasic Calcium Orthophosphates. In *Advanced Ceramic Materials*, Tiwari, A., Gerhardt, R.A., Szutkowska, M., Eds.; Scrivener Publishing: Beverly, MA, 2016; pp. 33-95.
16. Hsu, Y.-S.; Chang, E.; Liu, H.-S. Hydrothermally-grown monetite ($CaHPO_4$) on hydroxyapatite. *Ceram. Int.* **1998**, *24*, 249-254.
17. Gonzalez-McQuire, R.; Chane-Ching, J.-Y.; Vignaud, E.; Lebugle, A.; Mann, S. Synthesis and characterization of amino acid-functionalized hydroxyapatite nanorods. *J. Mater. Chem.* **2004**, *14*, 2277-2281.
18. Liu, J.; Li, K.; Wang, H.; Zhu, M.; Yan, H. Rapid formation of hydroxyapatite nanostructures by microwave irradiation. *Chem. Phys. Lett.* **2004**, *396*, 429-432.
19. Kong, X.-D.; Sun, X.-D.; Lu, J.-B.; Cui, F.-Z. Mineralization of calcium phosphate in reverse microemulsion. *Curr. Appl. Phys.* **2005**, *5*, 519-521.
20. Boonchom, B.; Danvirutai, C. The morphology and thermal behavior of calcium dihydrogen phosphate monohydrate ($Ca(H_2PO_4)_2{\cdot}H_2O$) obtained by a rapid precipitation route at ambient temperature in different media. *J. Optoelectron. Biomed. Mater.* **2009**, *1*, 115-123.

21. Liu, D.-M.; Yang, Q.; Troczynski, T.; Tseng, W.J. Structural evolution of sol–gel-derived hydroxyapatite. *Biomaterials* **2002**, *23*, 1679-1687.
22. Sivakumar, G.R.; Girija, E.K.; Narayana Kalkura, S.; Subramanian, C. Crystallization and characterization of calcium phosphates: Brushite and monetite. *Cryst. Res. Technol.* **1998**, *33*, 197-205.
23. Rohanizadeh, R.; LeGeros, R.Z.; Harsono, M.; Bendavid, A. Adherent apatite coating on titanium substrate using chemical deposition. *J. Biomed. Mater. Res., Part A* **2005**, *72A*, 428-438.
24. Djošić, M.S.; Mišković-Stanković, V.B.; Kačarević-Popović, Z.M.; Jokić, B.M.; Bibić, N.; Mitrić, M.; Milonjić, S.K.; Jančić-Heinemann, R.; Stojanović, J. Electrochemical synthesis of nanosized monetite powder and its electrophoretic deposition on titanium. *Colloids Surf. A Physicochem. Eng. Asp.* **2009**, *341*, 110-117.
25. Suchanek, W.L.; Shuk, P.; Byrappa, K.; Riman, R.E.; TenHuisen, K.S.; Janas, V.F. Mechanochemical–hydrothermal synthesis of carbonated apatite powders at room temperature. *Biomaterials* **2002**, *23*, 699-710.
26. Onoda, H.; Nakanishi, H. Preparation of calcium phosphate with oyster shells. *Nat. Resour.* **2012**, *3*, 71-74.
27. Macha, I.J.; Ozyegin, L.S.; Chou, J.; Samur, R.; Oktar, F.N.; Ben-Nissan, B. An alternative synthesis method for di calcium phosphate (monetite) powders from Mediterranean mussel (*Mytilus galloprovincialis*) shells. *J. Aust. Ceram. Soc.* **2013**, *49*, 122-128.
28. Karunadasa, K.S.P.; Manoratne, C.H.; Pitawala, H.M.T.G.A.; Rajapakse, R.M.G. Thermal decomposition of calcium carbonate (calcite polymorph) as examined by in-situ high-temperature X-ray powder diffraction. *J. Phys. Chem. Solids* **2019**, *134*, 21-28.
29. Seo, J.H.; Park, S.M.; Yang, B.J.; Jang, J.G. Calcined oyster shell powder as an expansive additive in cement mortar. *Materials* **2019**, *12*, 1322.
30. Seesanong, S.; Laosinwattana, C.; Boonchom, B. A simple rapid route to synthesize monocalcium phosphate monohydrate using calcium carbonate with different phases derived from green mussel shells. *J. Mater. Environ. Sci.* **2019**, *10*, 113-118.
31. Nakamoto, K. *Infrared and Raman Spectra of Inorganic and Coordination Compounds: Part A: Theory and Applications in Inorganic Chemistry*, 6th ed.; John Wiley & Sons: Hoboken, NJ, 2008.
32. Cotton, F.A. *Chemical Applications of Group Theory*, 3rd ed.; Wiley-Interscience: New York, NY, 1990.
33. Koura, N.; Kohara, S.; Takeuchi, K.; Takahashi, S.; Curtiss, L.A.; Grimsditch, M.; Saboungi, M.-L. Alkali carbonates: Raman spectroscopy, ab initio calculations, and structure. *J. Mol. Struct.* **1996**, *382*, 163-169.
34. Rahman, M.A.; Oomori, T. Structure, crystallization and mineral composition of sclerites in the alcyonarian coral. *J. Cryst. Growth* **2008**, *310*, 3528-3534.
35. Boonchom, B. Parallelogram-like microparticles of calcium dihydrogen phosphate monohydrate ($Ca(H_2PO_4)_2{\cdot}H_2O$) obtained by a rapid precipitation route in aqueous and acetone media. *J. Alloys Compd.* **2009**, *482*, 199-202.
36. Koleva, V.; Stefov, V.; Najdoski, M.; Cahil, A. Vibrational spectra of cobalt dihydrogen phosphate dihydrate, $Co(H_2PO_4)_2{\cdot}2H_2O$. *Vib. Spectrosc.* **2012**, *62*, 229-237.
37. Koleva, V.; Stefov, V. Phosphate ion vibrations in dihydrogen phosphate salts of the type $M(H_2PO_4)_2{\cdot}2H_2O$ (M=Mg, Mn, Co, Ni, Zn, Cd): Spectra–structure correlations. *Vib. Spectrosc.* **2013**, *64*, 89-100.
38. Xu, J.; F.R. Gilson, D.; S. Butler, I. FT-Raman and high-pressure FT-infrared spectroscopic investigation of monocalcium phosphate monohydrate, $Ca(H_2PO_4)_2{\cdot}H_2O$. *Spectrochim. Acta, Part A* **1998**, *54*, 1869-1878.
39. Rangavittal, N.; Landa-Cánovas, A.R.; González-Calbet, J.M.; Vallet-Regí, M. Structural study and stability of hydroxyapatite and β-tricalcium phosphate: Two important bioceramics. *J. Biomed. Mater. Res.* **2000**, *51*, 660-668.
40. Prevéy, P.S. X-ray diffraction characterization of crystallinity and phase composition in plasma-sprayed hydroxyapatite coatings. *J. Therm. Spray Technol.* **2000**, *9*, 369-376.